On the determination of cable characteristics for large dimension cable-driven parallel mechanisms

Nicolas Riehl, Marc Gouttefarde, Cédric Baradat and François Pierrot

Abstract— **Generally, the cables of a parallel cable-driven robot are considered to be massless and inextensible. These two characteristics cannot be neglected anymore for large dimension mechanisms in order to obtain good positioning accuracy. A well-known model which describes the profile of a cable under the action of its own weight allows us to take mass and elasticity into account. When designing a robot, and choosing actuator and cable characteristics, a calculation of maximal tension has to be done. However, because cable mass has a significant effect on cable tensions, a model including cable mass has to be included in the design step. This paper proposes two methods to determine the appropriate cable and hence the maximal tensions in the cables. Applied to a large dimension robot, taking cable mass into account is proved to be necessary in comparison with an equivalent method based on the massless cable modeling. In this paper, only moving platform static equilibria are considered (slow enough motions).**

I. INTRODUCTION

Parallel cable-driven robots consist mainly of a moving platform actuated by cables. The actuators are fixed to the base and drive spools around which the cables are wound, allowing the control of the position and orientation of the end effector by acting on the lengths of the various cables. Forces and torques can thereby also be transmitted to the platform.

One of the main drawbacks of cable-driven robots is that cables cannot transmit any force in compression, and thus must be kept under tension. Two main solutions exist to deal with this issue. Either, one or more additional cables than the n degrees of freedom (DOF) are used (fully constrained robots) [1] [2] [3], or as many cables as the number of DOF are used. In this latter case, sometimes referred to as cable suspended robots, the gravity acts as an additional vertical cable to keep the cables tensed [4] [5] [6].

Parallel cable mechanisms have several interesting characteristics in comparison to conventional parallel robots, such as reduced moving parts mass and inertia. This has been exploited in the high speed cable-driven parallel robot FALCON [7]. Additionally, the fact that cables are compliant makes parallel cable robots well adapted to human collaboration, e.g. in force feedback haptic interfaces [8] or for rehabilitation systems [9].

Another difference with conventional parallel robots comes from the possibility of storing large lengths of cables

N. Riehl and C. Baradat are with Fatronik France Tecnalia, Cap Omega Rond-point B. Franklin, 34960 Montpellier Cedex 2, France nriehl@fatronik.com, cbaradat@fatronik.com

M. Gouttefarde and F. Pierrot are with the Laboratoire d'Informatique, de Robotique et de Microélectronique de Montpellier (LIRMM), 161 rue Ada, 34392 Montpellier Cedex 5, France gouttefarde@lirmm.fr and pierrot@lirmm.fr

on spools. The possibilities in term of workspaces are thus almost unlimited. Several studies on large dimensions cable-driven robots have been made [4] [10] [11] [12] [13].

An important point in the study of parallel cable-driven robots is the modeling of cables. Since cables are not rigid bodies, their modeling is not straightforward. In most studies, cables are assimilated to rigid inextensible massless parts, provided they are tensed. Although this modeling is sufficient in several applications, it may be necessary to consider more realistic cable models. For instance, Behzadipour [14] has used a four spring system to model the stiffness of a single cable. Merlet also introduced elasticity in the modeling of the cables of the MARIONET robot [15].

Another modeling, that has not been extensively used for parallel cable robots, comes from civil engineering and more precisely from guyed bridge studies. Irvine [16] presented a single cable modeling taking cable mass and elasticity into account. Kozak used this modeling in the study of the large dimension telescope FAST [12] in order to compute the inverse kinematics of a very large cable suspended parallel robot. The effects of this model on the positioning accuracy of large dimension mechanisms has been shown to be important in [17] in which the effects of cable masses on the tensions in the cables have also been addressed. Actually, at some poses, taking into account cable mass can have a non-negligible effect on the maximal cable tension.

When designing and choosing cables and actuators, cable masses could have a significant influence. Indeed, the determination of the needed actuator torques and cable characteristics are notably based on the maximal tension in the cables across a desired workspace. Contrary to the case of massless cable modeling, the cable tension depends on the external forces acting on the cables but also on the own mass of the cable. Thus, the determination of the appropriate cable is not straightforward since it is based on the maximal tension which itself depends on some of the cable characteristics. This paper focuses on this issue and proposes two methods permitting the choice of the appropriate cable which will be able to withstand the maximal tension resulting from the platform mass and its own mass.

The well-known sagging cable modeling together with the formulation of the inverse kinematics problem are presented in section II. The differences between the massless and the sagging models regarding the determination of the cable tensions are discussed in section III. Two methods to determine, for a given pose, the appropriate cable will be proposed in section IV. Section V-A presents the application of this method to a whole workspace. In section V-B, the

Fig. 1.   Scheme of the platform and notations.

results obtained for a large dimension robot are presented and compared to those obtained when cable masses are not included in the model.

II. CABLE MODELING AND KINEMATICS

A. Massless inextensible cable model

In this kind of modeling, the cable is considered as a massless inextensible straight line. Thus, each leg of the cable robot is assimilated to a SPS mechanism, S denoting a spherical joint and P a prismatic joint, the prismatic joint being actuated.

The pose p (position $\mathbf{x}$ and orientation $\boldsymbol{\alpha}$) of the platform is expressed in the global fixed frame $\mathscr{R}_A(O_A, \boldsymbol{x}, \boldsymbol{y}, \boldsymbol{z})$. The position vector of the cable drawing point A_i with respect to frame $\mathscr{R}_A$ is denoted $\boldsymbol{a_i}$.

The positions of the cable attachment points B_i on the platform are expressed in the frame $\mathscr{R}_B(O_B, \boldsymbol{x_B}, \boldsymbol{y_B}, \boldsymbol{z_B})$ attached to the platform, O_B being the platform mass center. In the frame $\mathscr{R}_B$, the position vector of B_i is denoted $\boldsymbol{b_i}$. All these notations are gathered in Fig.1. The matrix $\boldsymbol{Q}$ is the rotation matrix from $\mathscr{R}_A$ to $\mathscr{R}_B$.

With the massless cable modeling, the inverse kinematics is straightforward. Indeed, the length l_i of the ith cable corresponds to the norm of the vector going from the drawing point A_i to the attachment point on the platform B_i. Let us denote $\boldsymbol{u_i}$ the unitary vector along the cable i from A_i to B_i.

The determination of the cable tensions has already been studied, e.g. [1] [18], and is thus not further detailed here.

B. Sagging model

1) Description of the model: This model describes the profile of the cable in the vertical plane containing A_i and B_i. Let us denote this plane $\mathscr{P}_i$ as shown in Fig.1. A frame $\mathscr{R}_i (A_i, \boldsymbol{x_i}, \boldsymbol{z_i})$ is attached to this plane. This frame shares the vector $\boldsymbol{z}$ with the frame $\mathscr{R}_A$. Thus, to transform $\mathscr{R}_A$ into the frame attached to the plane $\mathscr{P}_i$, one single rotation γ_i around $\boldsymbol{z}$ is needed as described in Fig. 2. The angle γ_i corresponds

to the angle between the projection of vector $\boldsymbol{u_i}$ on the $(\boldsymbol{x}, \boldsymbol{y})$ plane and the x-axis of the frame $\mathscr{R}_A$:

$$\gamma_i = \arctan\left(\frac{u_{iy}}{u_{ix}}\right) \tag{1}$$

where u_{ix} and u_{iy} correspond to the x and y coordinates of the vector $\boldsymbol{u_i}$ in the frame $\mathscr{R}_A$.

The associated rotation matrix is called $\boldsymbol{Q_i}$, and can be written as follows:

$$\boldsymbol{Q_i} = \begin{bmatrix} C\gamma_i & -S\gamma_i & 0 \\ S\gamma_i & C\gamma_i & 0 \\ 0 & 0 & 1 \end{bmatrix} = \begin{bmatrix} \boldsymbol{q_{i_1}} & \boldsymbol{q_{i_2}} & \boldsymbol{q_{i_3}} \end{bmatrix} \tag{2}$$

where $C\gamma_i$ and $S\gamma_i$ denote the cosine and sine of γ_i, respectively.

In the plane $\mathscr{P}_i$, a static cable model, presented in Irvine [16] for civil engineering and used by Kozak [12] in robotics, takes into account *cable mass and elasticity*. The cable does not have a linear profile as in the inextensible massless cable model, but sags under the action of its own weight as illustrated in Fig.3.

With this cable modeling, note that the force vector $\boldsymbol{\tau_{li}}$ applied at the end point B_i of cable i is not collinear to the vector $\boldsymbol{u_i}$. This force vector $\boldsymbol{\tau_{li}}$ can be projected on the x_i and z_i axes. The two resulting components are denoted F_{xi} and F_{zi}, as shown in Fig. 3.

In this model, the following mechanical cable characteristics are used: the young modulus E, the linear density ρ_0, and the unstrained section A_0. The cable profile is defined by (3) and (4) in which the coordinates x and z of a point on the cable with respect to the frame $\mathscr{R}_i$ are given as functions of the curvilinear abscissa s.

$$x_i(s) = \frac{F_{xi}s}{EA_0} + \frac{|F_{xi}|}{\rho_0 g}\left[\sinh^{-1}\left(\frac{F_{zi} + \rho_0 g(s - l_{0i})}{F_{xi}}\right)\right. \\ \left. - \sinh^{-1}\left(\frac{F_{zi} - \rho_0 g l_{0i}}{F_{xi}}\right)\right] \tag{3}$$
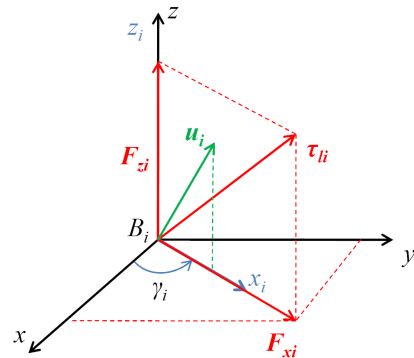
Fig. 2.   Relationship between the fixed frame and the frame attached to the cable.
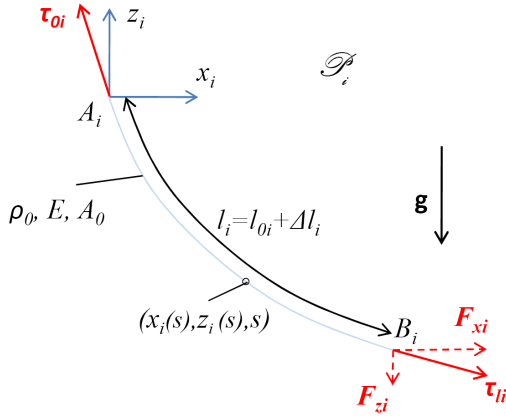
Fig. 3. Cable i in the plane $\mathscr{P}_i$ with the "sagging" cable modeling.

$$z_i(s) = \frac{F_{zi}s}{EA_0} + \frac{\rho_0 g}{EA_0}\left(\frac{s^2}{2} - l_{0i}s\right)$$
$$+ \frac{1}{\rho_0 g}\left[\sqrt{F_{xi}^2 + (F_{zi} + \rho_0 g\,(s - l_{0i}))^2}\right.$$
$$\left. - \sqrt{F_{xi}^2 + (F_{zi} - \rho_0 g l_{0i})^2}\right] \quad (4)$$

2) Inverse kinematics: With this sagging cable modeling, it is not straightforward to determine the length of each cable for a given pose of the platform. Actually, the cable lengths are completely coupled to the forces applied to the cables. Thus, these variables (cable lengths and applied forces) have to be determined at the same time. The unknowns are the unstrained lengths l_{0i} of the n cables and the components F_{xi} and F_{zi}, in the frame $\mathscr{R}_i$, of the force τ_{li} applied to the cable at B_i as shown in Fig.3. The unknowns are thus:

$$\begin{bmatrix} F_{x1} & F_{z1} & l_{01} & \cdots & F_{xn} & F_{zn} & l_{0n} \end{bmatrix}_{1\times 3n} \quad (5)$$

In order to determine these unknowns at least $3n$ equations arer required. First, in (3) and (4), by replacing the curvilinear abscissa s by the length l_{0i} of cable i, $x(l_{0i})$ and $z(l_{0i})$ correspond to the coordinates of the point B_i with respect to the frame $\mathscr{R}_i$. Let us denote this coordinate vector x_i which is defined as:

$$x_i = \begin{bmatrix} x(l_{0i}) \\ 0 \\ z(l_{0i}) \end{bmatrix} = Q_i^{-1}\left(\mathbf{x} + Qb_i - a_i\right) \quad (6)$$

Thereby, we get $2n$ non-linear equations:

$$x(l_{0i}) = \frac{F_{xi}l_{0i}}{EA_0} + \frac{|F_{xi}|}{\rho_0 g}\left[sinh^{-1}\left(\frac{F_{zi}}{F_{xi}}\right)\right.$$
$$\left. - sinh^{-1}\left(\frac{F_{zi} - \rho_0 g l_{0i}}{F_{xi}}\right)\right] \quad (7)$$

$$z(l_{0i}) = \frac{F_{zi}l_{0i}}{EA_0} - \frac{l_{0i}^2 \rho_0 g}{2EA_0} + \frac{1}{\rho_0 g}\left[\sqrt{F_{xi}^2 + F_{zi}^2}\right.$$
$$\left. - \sqrt{F_{xi}^2 + (F_{zi} - \rho_0 g l_{0i})^2}\right] \quad (8)$$

The other n equations are those of the platform static equilibrium:

$$W_f f = e \quad (9)$$

where

$$f = \begin{bmatrix} F_{x1} & F_{z1} & \cdots & F_{xn} & F_{zn} \end{bmatrix}^t_{2n\times 1}$$

$$e = \begin{bmatrix} mg \\ 0 \end{bmatrix}_{6\times 1}$$

$$W_f = \begin{bmatrix} q_{1_1} & q_{1_3} & \cdots \\ Qb_1 \times q_{1_1} & Qb_1 \times q_{1_3} & \cdots \\ \cdots & q_{n_1} & q_{n_3} \\ \cdots & Qb_n \times q_{n_1} & Qb_n \times q_{n_3} \end{bmatrix}_{6\times 2n}$$

where m is the platform mass, g the gravitational acceleration vector, b_{ix}, b_{iy} and b_{iz} the components of vector b_i, i.e. the coordinates of B_i in $\mathscr{R}_B$, and where q_{i_j} is the jth column of matrix Q_i as defined in (2).

III. CABLE TENSIONS FOR DESIGN

In the context of the design of large workspace cable-driven robots, besides the workspace, one of the main aspects to take into account is the actuator capabilities. Actually, the actuator has to be able to support the maximal cable tension all over the desired workspace. This maximal tension is also involved in the proper determination of the cable. After the choice of the cable structure (number and layout of threads) and its material, considering the elasticity and other material characteristics, an important parameter to choose is the diameter. The cable diameter can be chosen directly from the maximal tension. In fact, for most cables, the maximal supported tension is proportional to the section of the cable. When the massless cable model is used, the determination of the appropriate cable and actuator can be done by determining the maximal tension that can occur in the cable over the whole workspace.

But, when cable mass is taken into account, sagging appears. Kozak [12] has shown that sagging have effects on the positioning of the platform. But, cable tension is also significantly affected by the mass of the cables [17]. Actually, the actuator and the cable have to support a part of the platform mass, but also the mass (or a part of it) of the hanging cable. Thus, while taking cable mass into account, the maximal tension τ_{imax} will be higher than with the simple model of cable, since:

$$\tau_{imax} = \sqrt{F_{xi}^2 + (F_{zi} - \rho_0 g l_{0i})^2}. \quad (10)$$
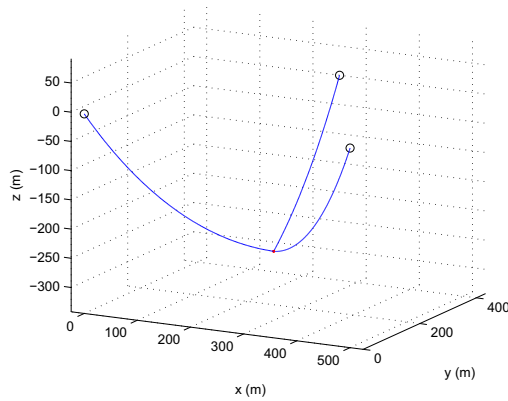
Fig. 4.   3 DOF / 3 cables point mass cable-driven mechanism.

Note that, in this paper, F_{zi} is considered to be negative in (10) (poses at which a cable is hanging below the platform are disregarded).

The problem here is that the tension in the cable is directly dependent on the cable mass and thus on the cable section. Therefore, when choosing a cable section to support the maximal tension, the increase of cable diameter will induce an increase of cable tension and so on, a larger cable section will be needed. The next section shows that a "fixed point" seems to exist.

IV. CABLE SECTION DETERMINATION METHODOLOGY

A. Description of the robot studied

The robot considered in that study is a point mass cable suspended robot, that is to say, a 3 cables / 3 DOF robot in which gravity keeps cables under tension. The 3 DOF are the three translations along the x, y and z axes. The 3 cable exit points are located at the 3 extremities of an equilateral triangle. The dimensions of the structure have been chosen to allow us to see the effect of cable mass. In fact, the dimensions have been chosen to be the same as the mechanism FAST studied by Kozak [12]. Thus, the positions of the exit points of each cable, expressed in the fixed frame, are given in TABLE I. The end effector mass has been chosen to be 4000Kg.

The type of cable chosen for that study is made of galvanized steel in a 7×19 threads structure. The corresponding density M_v is of 7800Kg/m^3 considering the cable as a cylinder. From the breaking loads given for different cable diameters by the manufacturers, the corresponding maximal

TABLE I

EXIT POINTS POSITIONS

	x (m)	y (m)	z (m)
a_1	0	0	0
a_2	500	0	0
a_3	250	433.01	0

admissible stress σ_{max} results to be 180MPa using a safety factor of 2. This value is based on the yield strength of such material. The Young modulus of the cable is 200GPa.

B. Basic loop method

In this section, the first methodology used to determine the cable section needed for a given mechanism and application is presented. The robot geometry is assumed to be known.

1) Methodology: For a given pose, we start by using the massless cable model to determine the maximal tension, and we deduce the cable section from this value. Once this step realized and the cable characteristics known, we can compute the inverse kinematics of the manipulator with the sagging model. We obtain a new value of the maximal tension higher than the one found with the massless model because of the cable mass now taken into account. Thus, we find a new value of the cable diameter. We then reproduce this procedure as many time as needed to reach a diameter variation Δ_{diam} inferior to a given threshold ε. This procedure followed here is described schematically in Fig.5.
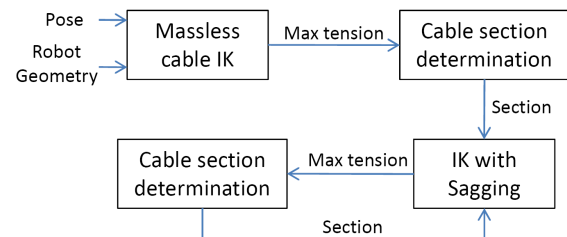
Fig. 5.   Cable characteristic determination loop.

2) Results for a given pose: For the manipulator of TABLE I, this procedure is applied to the pose $[250, 200, -50]$, with a platform mass of 4000Kg. The results in terms of cable tension and corresponding cable diameter are presented in Fig.6 and Fig.7, respectively.

It can be noticed that these values are converging in just a few iterations with $\varepsilon = 10^{-6}$m. In this example, the
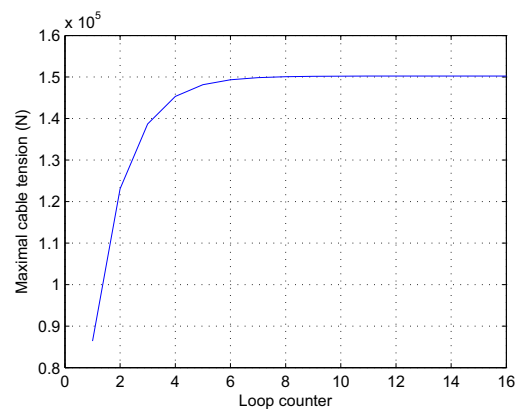
Fig. 6.   Maximal cable tension evolution along the loop.
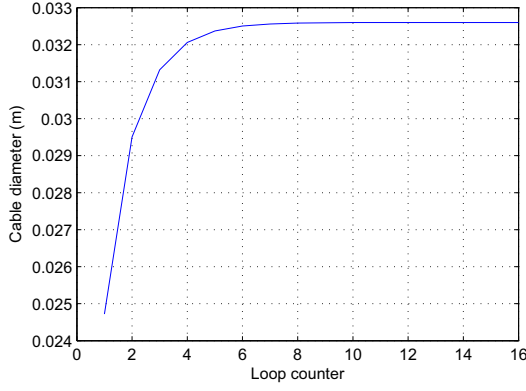
Fig. 7. Cable diameter evolution along the loop.

appropriate cable appears to be of diameter 32.6mm. The maximal tension reaches 150.2KN. That is to say, at the considered pose, the cable with a diameter of 32.6mm will withstand the tension due to both the end-effector and the cable mass.

C. Determining the appropriate cable by optimization

In this subsection, another method to determine the appropriate cable section is proposed. This method is based on an optimization integrated to the inverse kinematics computation.

1) Methodology: The inputs to our problem are the description of the structure, that is to say the position of the cable exit points, the platform description (attachment points and mass) and the pose (position and orientation) of the platform. Our goal is to determine simultaneously the length of each cable, the forces exerted by the cables on the platform for the latter to be in static equilibrium, and the cable section.

Actually, the criterion to minimize is the cable diameter with the constraint of being able to support the tensions due to the platform mass and also to the cable own mass.

Thus, in the optimization, the non-linear constraints are given by the static equilibrium of the platform described in (9), and by the cable profile equations of the sagging model (7) and (8).

In (7) and (8), the section of the cable A_0 can be replaced by its expression as a function of the linear density ρ_0 of the cable, since the cable material is chosen (galvanized steel). The Young modulus E and its density M_v are also known. Equations (7) and (8) become:

$$
x(l_{0i}) = \frac{F_{xi}l_{0i}M_v}{E\rho_0} + \frac{|F_{xi}|}{\rho_0 g}\left[sinh^{-1}\left(\frac{F_{zi}}{F_{xi}}\right) \right.
$$
$$
\left. - sinh^{-1}\left(\frac{F_{zi} - \rho_0 g l_{0i}}{F_{xi}}\right) \right] \tag{11}
$$

$$
z(l_{0i}) = \frac{F_{zi}l_{0i}M_v}{E\rho_0} - \frac{l_{0i}^2 g M_v}{2E} + \frac{1}{\rho_0 g}\left[\sqrt{F_{xi}^2 + F_{zi}^2} \right.
$$
$$
\left. - \sqrt{F_{xi}^2 + (F_{zi} - \rho_0 g l_{0i})^2} \right] \tag{12}
$$

Thus, the unknowns of the problem, gathered in the vector shown in (13), are the 6 cable lengths, the forces exerted on cable i along the axes x_i and z_i of the frame $\mathscr{R}_i$ (Fig.1) and the linear density ρ_0 of the cables.

$$
\begin{bmatrix} F_{x1} & F_{z1} & l_{01} & \cdots & F_{xn} & F_{zn} & l_{0n} & \rho_0 \end{bmatrix}_{1\times(3n+1)} \tag{13}
$$

Inequality constraints are also added. Since the material and the structure of the cables are known, the maximal stress each cable can withstand σ_{max} is also known. Using a safety factor k, an inequality on the resistance of the cables can be expressed as follows:

$$
\frac{k\tau_{0i}}{A_0} \le \sigma_{max} \qquad \forall i = 1\ldots n \tag{14}
$$

2) Results for a given pose: Considering the same pose used for the basic loop method, i.e. $[250, 200, -50]$, the optimization presented before is computed, and the optimized cable diameter obtained is 32.6mm. This result confirms the one given with the basic loop method and validates these two methods, at least for the example at hand.

V. APPROPRIATE CABLE DETERMINATION ACROSS A WORKSPACE

A. Principle and methodology

The two methods presented in the previous section allow us to determine the appropriate cable for a given robot geometry and a given pose. The next step is to be able to find the pose in the workspace where the tension is the highest, and thus where the needed cable is the thickest. The first idea was to use the massless model to determine, by sampling the whole workspace, the pose where the tension is the highest. But, on the one hand, finding such a pose is not an easy task and, on the other hand, nothing guarantees that this pose would also be the one with the highest tension while taking cable mass and elasticity into account. Furthermore, it is neither obvious that this pose will be the one which requires the thickest cable.

Therefore, the method presented in section IV-C is applied to each pose of the sampled workspace. The resulting largest cable diameter should be very close to the one required across the whole workspace (for a fine enough discretization).

B. Results and analysis

The geometry of the robot under study is given in TABLE I. The sampled workspace corresponds to the volume limited by the three posts and, along the z axis, located between -200m and -40m. At each pose, the optimization presented in section IV-C has been computed, and, thereby, a mapping

Fig. 8. Appropriate cable diameters all over the workspace.
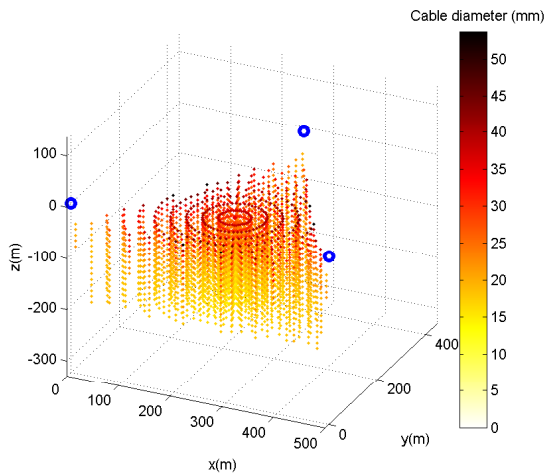
Fig. 9. Appropriate cable diameters in the plane z=-40m.

of the required cable diameters all over the workspace is obtained and presented in Fig.8.

It can be noted in this figure that the maximal cable diameters, and thus the maximal tensions, are found on the upper part of the workspace. This can be explained by the fact that the higher the pose is in the workspace, the more horizontal the cable are, and so the higher the cable tensions are to balance the vertical force produced by the end effector mass. Fig.9 shows the diameters obtained for the upper part of the workspace.

In this figure, the poses where the cable tensions are the highest are seen to be located on the boundaries of the triangle formed by the three posts. The corresponding appropriate cable diameter is 51.2mm. This value corresponds to a maximal tension of 371kN.

With the same robot and using massless cable modeling, the maximal tension would have been 121kN yielding a cable diameter of 29.3mm. Thus, this results in a significant error since the real tension is about three times higher.

VI. CONCLUSIONS

This paper deals with the choice of cables for large scale cable-suspended robots taking cable masses and elasticity into account. After presenting a formulation of the inverse kinematics problem, based on a well-known static cable modeling, two methods are proposed to determine, for a n cable/n DOF parallel cable-driven robot, the appropriate cable that can withstand the tensions due to both the mobile platform mass and the cable own mass. Based on a discretization, these methods enable the exploration of a given workspace. These methods applied to a large scale cable-suspended robot are proved to be necessary in comparison with a determination based on a massless cable modeling.

REFERENCES

[1] C. Ferraresi, "A new methodology for the determination of the workspace of six-dof redundant parallel structures actuated by nine wires," *Robotica*, vol. 25, pp. 113–120, 2007.
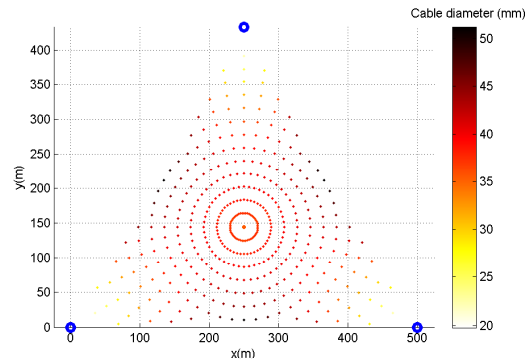
[2] P. Bosscher, "Cable-suspended robotic contour crafting system," *Automation in Construction*, vol. 17, pp. 45–55, 2006.

[3] K. Maeda, S. Tadokoro, T. Takamori, M. Hiller, and R. Verhoeven, "On design of a redundant wire-driven parallel robot WARP manipulator," in *Proceedings of IEEE International Conference on Robotics and Automation, ICRA 1999*, Detroit, MI, USA, 1999, pp. 895–900.

[4] J. Albus, R. Bostelman, and N. Dagalakis, "The NIST robocrane," *Journal of Robotic Systems*, vol. 10, no. 2, pp. 709–724, 1993.

[5] A. B. Alp and S. K. Agrawal, "Cable suspended robots: design, planning and control," in *Proceedings of IEEE International Conference on Robotics and Automation, ICRA 2002*, 2002, pp. 4275–4280.

[6] S.-R. Oh and S. K. Agrawal, "Cable-suspended planar parallel robots with redundant cables: controllers with positive cable tensions," in *Proceedings of IEEE International Conference on Robotics and Automation, ICRA 2003*, Sept. 2003, pp. 3023–3028.

[7] S. Kawamura, W. Choe, S. Tanaka, and S. R. Pandian, "Development of an ultrahigh speed robot FALCON using wire-driven system," in *Proceedings of IEEE International Conference on Robotics and Automation, ICRA 1995*, Nagoya, Japan, May 1995, pp. 215–220.

[8] Williams, "Cable suspended haptic interface," *International Journal of Virtual Reality*, vol. 3, pp. 13–21, 1998.

[9] R. C. V. Loureiro, C. F. Collin, and W. S. Harwin, "Robot aided therapy: challenges ahead for upper limb stroke rehabilitation," in *International Conference on Disability, Virtual Reality and Associated Technologies*, 2004.

[10] S. Havlik, "A cable-suspended robotic manipulator for large workspace operations," *Comput. Aided Civil Infrastruct. Eng.*, vol. 15, pp. 56–68, 2000.

[11] P. Bosscher and I. Ebert-Uphoff, "Disturbance robustness measures for underconstrained cable-driven robots," in *Proceedings of IEEE International Conference on Robotics and Automation, ICRA 2006*, Orlando, FL, May 2006, pp. 4205–4212.

[12] K. Kozak, Q. Zhou, and J. Wang, "Static analysis of cable-driven manipulators with non-negligible cable mass," *IEEE Transactions on Robotics*, vol. 22, pp. 425–433, June 2006.

[13] R. Nan and B. Peng, "A chinese concept for 1km radio telescope," *Acta Astronautica*, vol. 46, pp. 667–675, 2000.

[14] S. Behzadipour, "Stiffness of cable-based parallel manipulators with application to stability analysis," *Journal of mechanical design*, vol. 128, pp. 303–310, Janvier 2006.

[15] J.-P. Merlet, "Kinematics of the wire-driven parallel robot marionet using linear actuators," in *Proceedings of IEEE International Conference on Robotics and Automation, ICRA 2008*, Pasadena, CA, May 2008, pp. 3857–3862.

[16] H. Irvine, *Cable structures*. Cambridge, MA: MIT Press, 1981.

[17] N. Riehl, M. Gouttefarde, S. Krut, C. Baradat, and F. Pierrot, "Effects of Non-Negligible Cable Mass on the Static Behavior of Large Workspace Cable-Driven Parallel Mechanisms," in *Proceedings of IEEE International Conference on Robotics and Automation, ICRA 2009*, May 2009, pp. 2193–2198.

[18] R. G. Roberts, T. Graham, and T. Lippitt, "On the inverse kinematics, statics, and fault tolerance of cable-suspended robots," *Journal of Robotic Systems*, vol. 15, pp. 581–597, 1998.